Formation of Oxygen Induced Nanopyramids on Rh(210) Surface

Govind[a]*, Wenhua Chen[b], Hao Wang[b] and T.E. Madey[b]

[a]*Surface Physics and Nanostructures Group, National Physical Laboratory, Dr. K.S. Krishnan Road, New Delhi -110012 (India))*
[b]*Department of Physics & Astronomy and Laboratory for Surface Modification, Rutgers, The State University of New Jersey, 136 Frelinghuysen Road, Piscataway, NJ 08854, USA*

Abstract. Formation of oxygen induced nano pyramids on atomically rough and morphological unstable Rh (210) surface has been studied using Auger electron spectroscopy (AES), low energy electron diffraction (LEED), and UHV-scanning tunneling microscopy (STM). Nanometer sized pyramids can be formed upon annealing the oxygen-covered Rh (2 1 0) surface at ≥600K in the presence of oxygen (10^{-8} Torr) and the facets of the pyramids are identified as two {731} face and a (1 1 0) face. The study suggests that the oxygen overlayer can be removed from the surface via catalytic reaction at low temperature using CO oxidation while preserving ("freezing") the pyramidal facet structure. The resulting clean faceted surface remains stable for *T*~600 K and for temperatures above this value, the surface irreversibly relaxes to the planar state. Atomically resolved STM measurements confirm the formation of nanopyramids with average pyramid size ~18nm. The nanopyramidal faceted Rh surface will be used as nanotemplates for growth of nanometer-scale clusters.
Keywords: Faceting, Rhodium, Low energy electron diffraction (LEED), Auger Electron Spectroscopy (AES), Scanning Tunneling Microscopy (STM)
PACS: 68.47, 68.43, 68.37

INTRODUCTION

Atomically rough clean metal surfaces generally have lower surface atom density and higher surface free energy than close-packed surfaces of the same metal. A variety of atomically-rough clean metal surfaces can be prepared as stable orientations, but the presence of (strongly interacting) adsorbates can cause changes in surface morphology through mechanisms such as reconstruction and facet formation [1–6]. These morphological changes are usually explained in terms of changes in surface free energy due to the presence of adsorbate [7,8]. Many studies have been performed on adsorbate induced faceting of atomically rough surfaces, e.g., bcc W(111), Mo(111), fcc Cu(210), Ir(210), Pt(210) and Ni(210) and hcp Re (12-31) and Re(11-21) surfaces [3-11].

In the present study, we focus on the fcc Rh (210) surface which is an important substrate for catalytic processes and has potential applications in surface chemistry. We study the oxygen induced morphological change of Rh(210) surface. Previous studies on other fcc (210) surfaces [5-9] indicate that the facets can be induced due to the presence of various gaseous adsorbates for example oxygen and

CPU 47, *Transport and Optical Properties of Nanomaterials—ICTOPON - 2009*, edited by M. R. Singh and R. H. Lipson

nitrogen can induce faceting of Cu (210) and Ni(210) while oxygen and CO provide favorable conditions to restructure the Pt (210) surface to form facets. Ir (210) [8] shows the formation of pyramidal type facets with {311} and (110) facets, when annealed in the presence of oxygen above 600K.

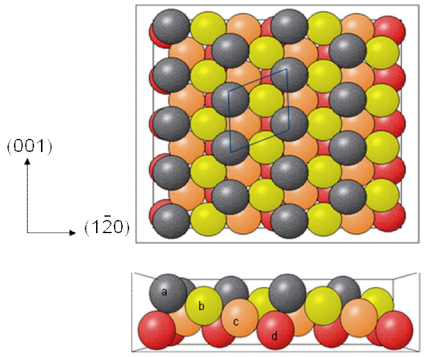

FIGURE 1. Hard sphere model of fcc (210) surface (top & side view) showing top four exposed layer

The Rh (210) surface is atomically rough; as shown in figure 1, the unreconstructed Rh (210) has four layers of atoms exposed and the top layer of the atoms shows mirror reflection symmetry along $(\bar{1}20)$ plane. Here, we study the morphological changes induced by oxygen on Rh (210) and formation of nanopyramids. The nanofaceted surface is characterized by LEED, AES and STM.

EXPERIMENTAL DETAILS

The experiments were carried out in two different ultrahigh vacuum (UHV) chambers denoted as LEED and STM chambers respectively. All LEED images are obtained in the LEED chamber that also contains a quadrupole mass spectrometer (QMS) for residual gas analysis and a cylindrical mirror analyzer for AES. STM experiments described herein were performed in the STM chamber at room temperature using a hybrid variable temperature Omicron STM with tungsten tips. The Rh(210) crystal is cut from a single crystal Rh (99.99%) rod ~10 mm in diameter, ~1.5 mm thick, aligned within 0.5^{o} of the (210) orientation and polished to a mirror finish. The sample is supported by two rhenium leads where a high current (up to 30A) can be passed through the leads to achieve temperatures up to 1600K. A C-type (W–5 at.% Re/W–26 at.% Re) thermocouple is spot welded directly to the rear of the sample for accurate temperature measurement. The sample support assembly also includes a tungsten filament for electron bombardment heating; a temperature up to 2000K can be achieved by flashing the sample in UHV. The sample was cleaned by repeated cycles of Argon ion bombardment (1keV, 3.5μA) at 300-650K (initially at 300K and then at increasingly higher temperature (<650K), annealing in UHV at 1200K, annealing in O_2 ($2x10^{-8}$ Torr) at 1000 -1200K followed by rapid flashes to ~1600K in UHV to desorbs the excess oxygen from the surface. The oxygen gas deposition was achieved by back-filling the chamber using research purity O_2 at background pressures $2x10^{-8}$ Torr for different time depending on the desired dose.

CPU 47, *Transport and Optical Properties of Nanomaterials—ICTOPON - 2009*, edited by M. R. Singh and R. H. Lipson

RESULTS

A typical LEED pattern obtained from the clean fcc Rh(2 1 0) surface is shown in Fig. 2a. The spots observed by LEED are consistent with the LEED pattern of an unreconstructed bulk fcc (2 1 0) plane. When electron beam energy (Ee) is increased the electron wavelength and, consequently, the diffraction angles decrease, and an apparent motion of the diffraction beams toward the specularly reflected (0,0) beam is observed. For the clean Rh(2 1 0) surface the (0,0) beam is perpendicular to the macroscopic surface plane and is in the center of the LEED pattern. This behavior of the LEED beams is an indication that the surface is both macroscopically and microscopically planar. No new beams appear in the LEED pattern as a result of oxygen adsorption at room temperature. However, the intensity of this background signal increases with exposure and is attributed to additional diffuse scattering from the oxygen overlayer and oxygen induced disorder in the topmost Rh layer. The behavior of the oxygen covered Rh(210) surface show significant changes on annealing the substrate to higher temperature. The LEED pattern gradually changes with temperature. As the sample temperature is slowly increased LEED beams of the initial (1 x 1) pattern diffuse and, seemingly, elongate in three different directions or three additional elongated beams appear around them. The transition between a clearly (1 x 1) pattern and the diffuse one is very gradual and it is difficult to pinpoint accurately the temperature at which it occurs; the lowest temperature at which the pattern is clearly different from the original (1 x1) is approximately 450 K. With further temperature increase the (1 x1) beams become progressively fainter, and the emerging new beams become gradually brighter and sharper. This process continues until the sample temperature has reached 600 K, when all trace of the (1 x 1) beams has disappeared, including the specularly reflected (0, 0) beam and a pattern appeared with a completely different geometry and roughly three times more spots than planar surface. The geometry of the LEED pattern does not change with further (above 600 K) temperature increase. Subsequent cooling of the sample to room temperature does not reverse the process and the new pattern remains stable and unchanged in the entire temperature range. For experiments performed without oxygen in the background gas surface cleanliness is critical: carbon contamination can impede or even completely prevent the occurrence of the described transformations. When Ee is varied the behavior of the new LEED pattern differs from that of the (1x1) (Fig. 2c) rather than converging on the center of the pattern, the diffracted beams move in directions that converge to three distinct position. Three LEED beams (labeled by small circles in the figure 2b & 2c) can be observed, each coinciding with one of the three convergence points. They can therefore be identified as specular reflection beams originating from surfaces that are tilted with respect to the (2 1 0) macroscopic surface plane. Moreover, the complete LEED pattern is the superposition of three distinct LEED patterns, whose respective specular directions are each inclined at unique angles (with respect to the macroscopic crystal plane), determined by the crystallographic orientation of the surfaces from which they originate. LEED patterns with similar revealing characteristics have been previously observed in similar experiments, involving oxygen and metallic overlayers on W(1 1 1) [3,4,12]. Subsequently, the

CPU 47, *Transport and Optical Properties of Nanomaterials—ICTOPON - 2009*, edited by M. R. Singh and R. H. Lipson

emergence of these patterns has been interpreted to be a consequence of the formation of nanometer-size facets on the substrate surface.

The crystallographic orientation of these facets can be determined by calculating the corresponding facet tilt angles with respect to (210) plane, and the azimuthal orientation of facets with respect to each other. We calculate the tilt angle between a facet plane corresponding to the specular beam A & B and the normal direction of the (210) plane which is 8 ± 0.5^{o}[13]. The azimuthal angle between these two faceted planes can be directly measured and is $\Phi = 132\pm4^{o}$. The tilt angle between the third facet, defined by the specular beam position C in figure 2(b) and the normal direction of the (210) plane is also calculated in similar manner. However, from figure 2(b), the exact position of the specular beam from third facet is difficult to observe as the specular beam corresponding to this facet is blocked by the leads of the sample support assembly. The estimated tilt angle between the facet and the normal direction of the (210) plane is found to be 18 ± 2^{o}. Based on the tilt angle between the faceted plane and (210) plane as well as azimuthal angle between the two symmetric facets, the Miller indices of first two facets are identified as (731) and $(73\bar{1})$ planes and while the third facet is identified as (110) facet [13]. The observation of {731} and (110) facet is also supported by early study by Tucker [14] on Rh (210) surface. However, Tucker observed diffraction spots corresponding to {731} facet on Rh (210) when annealing the surface in oxygen background $1x10^{-7}$ Torr at 573K and these diffraction spot are completely replaced by (110) plane when annealing in oxygen pressure $1x10^{-6}$ Torr at the same temperature.

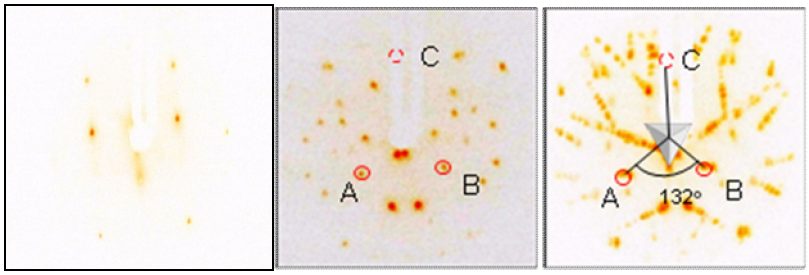

(a) (b) (c)

FIGURE 2: (a) LEED pattern from a clean surface of Rh(210) at incident electron beam 80eV (b) LEED pattern from faceted O/Rh(210) at electron beam energy 66eV(c) LEED pattern for electron beam energy 20-74ev. The pyramid in c illustrates the origin of the specular beams and azimuthal angle used to determine the facet.

The production of a clean or freezing of the facets is a new aspect to overlayer-induced faceting experiments of the faceted rhodium surface. From the literature the most straightforward method of removing oxygen from the rhodium surface is through thermal desorption, however, to produce a clean faceted rhodium surface is difficult because the faceted surface reverts to planar at 600 K (in the absence of oxygen background). This temperature is significantly lower than those required to completely remove the oxygen by desorption (~1400 K) making it impossible to remove the oxygen by desorption without destroying the faceted surface. However, our investigations have revealed that it is possible to chemically removing the oxygen overlayer at low temperature. For this we used the method to takes advantage of

CPU 47, *Transport and Optical Properties of Nanomaterials—ICTOPON - 2009*, edited by M. R. Singh and R. H. Lipson

catalytic CO oxidation in the following manner: commencing with a faceted surface (Fig. 3a) completely covered with oxygen, the temperature of the sample is set to 390 K and then CO is leaked into the chamber at a pressure of 4 $x10^{-9}$ Torr. As expected (Eq. (1)), a surface reaction occurs,

$$CO_{(ad)} + O_{(ad)} \text{ ----------} CO_{2(g)} \qquad (1)$$

which results in an increase of the CO_2 signal in the residual gas mass spectrum. When the integrated CO dose has reached 0.48 L (after ~120 s) the CO is pumped from the chamber and the sample temperature is increased further (to 450 K) and held at that temperature (in UHV) for additional 2 min, in order to desorbs any excess CO. Upon cooling to room temperature the surface retains its faceted structure, as verified by LEED (Fig. 3b). AES studies confirm that an atomically clean faceted surface has been produced (Fig. 3c).

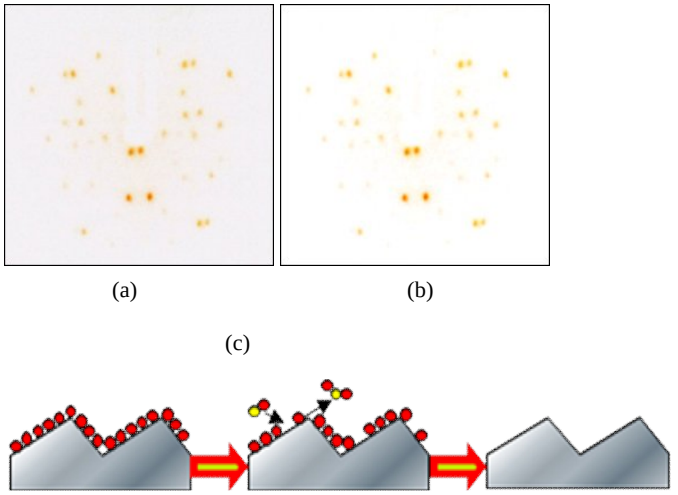

FIGURE 3: LEED pattern form the faceted Rh(210) at electron energy 90eV. (a) oxygen–covered faceted surface and (b) clean faceted surface (c) illustrate the cleaning reaction

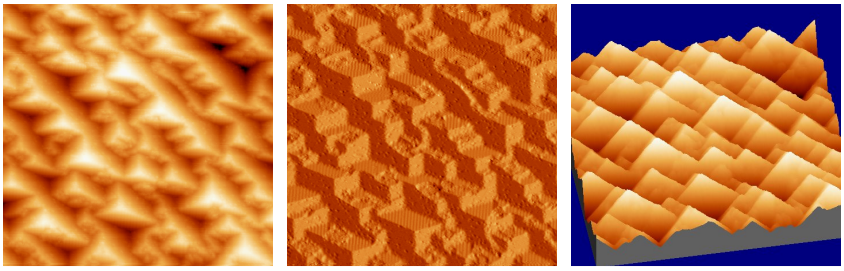

FIGURE 4: STM scan of the fully faceted Rh (210) surface by annealing to 850K and cooling to room temperature in oxygen background (a) The STM image of the nanopyramidal faceted surface san area 100nmx100nm (a) STM image of faceted Rh(210) surface with scan area 100nmx100nm (b) X-slope image with scan area 100nmx100nm, V=1.2mV, I=1nA (c)3D image of nanopyramids with facets of (731), (73-1) and reconstructed (110) surface

Figure 4(a) shows a typical STM image of faceted Rh (210) surface prepared by pre dosing of 10L oxygen at 300K followed by annealing at 850K for 2 min followed by cooling to 300K in the presence of oxygen ($4x10^{-8}$ Torr) [13]. The faceted Rh surface is fully covered with well formed nano pyramids (three sided

CPU 47, *Transport and Optical Properties of Nanomaterials—ICTOPON - 2009*, edited by M. R. Singh and R. H. Lipson

facets) with similar shape, which implies that they expose faces of identical crystal orientation. To reveal the atomic details, we differentiate the height of STM images along x-direction (x-slope); with this procedure the details of STM images can be enhanced at the cost of losing height information. The three dimensional image of the faceted surface is presented in figure 4(c).The orientation of the facets identified by LEED can be further confirmed by measuring azimuthal angles between the edge lines of each of the facet. The average pyramid size for the above surface is found to be ~18nm. The size of the nanopyramids can vary from 12nm to 21 nm, depending upon the annealing temperature. The biggest average nano pyramid size can be obtained by flashing the Rh (210) surface in the presence of oxygen to 1600K. These nanopyramids can be used as a template to grow metallic nanoclusters and biological molecules.

CONCLUSION

In the present work, we focus on the adsorbate induced modification of the surface morphology of the Rh(210) substrate. We observed oxygen induced pyramidal faceting of Rh(210) surface with {731} and (110) facets when annealing Rh(210) in O_2 The average pyramid size ranges from 12nm to 21nm, which can be controlled by changing the annealing temperature from. The faceted Rh surfaces provide possible model systems to study structure sensitivity in Rh based catalytic reactions as well as potential nanotemplate to grow nanoclusters.

ACKNOWLEDGMENTS

This work has been supported by the U.S. Department of Energy (DOE), Office of Basic Energy Sciences (Grant DE-FG-02-93ER14331). Dr. Govind thanks Department of Science & Technology, Govt. India, New Delhi, India for BOYSCAST fellowship.

REFERENCES

1. G. Ertl; H. Knozinger; J. Weitkamp, Handbook of Heterogeneous Catalysis (Wiley, New York) 1997
2. Q. Chen, N. V. Richardson, Surface, *Prog. Surf. Sci.* 2003, *73*, 59–77
3. T.E. Madey; J.Guan; C. H. Nien; C. Z. Dong ; H. S. Tao; R.A. Campbell, *Surf. Rev. Lett.* 1996, *3*, 1315-1328
4. T.E. Madey; C.H. Nien; K. Pelhos; J.J. Kolodziej; I.M. Abdelrehim; H. S. Tao. *Surf. Sci.*, *438*, 191-206 (1999)
5. R. E.Kirby; C. S. McKee; M. W. Roberts, *Surf. Sci.*, *55*, 725–728. (1976)
6. R. E. Kirby; C. S. McKee; L. V. Renny, *Surf. Sci.*, *97*, 457–477 (1980)
7. A. T. S. Wee;, J. S. Foord; R. G. Egdell,; J. B. Pethica, *Phys. Rev. B*, *58*, R7548-R7551 (1998)
8. I. Ermanoski; K. Pelhos; W. Chen; J. S. Quinton; T. E. Madey, *Surf. Sci.*, *549*, 1–23. (2004)
9. M. Sander; R. Imbihl; R. Schuster; J. V. Barth; G. Ertl, *Surf. Sci.*, *271*, 159–169 (1992)
10. H. Wang; W. Chen; T. E. Madey, *Phys. Rev. B 74*, 205426. (2006)
11. H. Wang, A.S.Y Chan, W. Chen, P. Kaghazchi, T. Jacob and T. E. Madey *ACS Nano,1(5)* 449-455 (2007)
12. K.J. Song, J. C. Lin, M. Y. Lai, Y. L. Wang, Surf. Sci. 327, 17(1994)
13. Govind, Wenhua Chen, Hao Wang and T.E. Madey (communicated)
14. C.W. Tucker Jr., *Acta Metallurgica* 1967,*15*, 1465

CPU 47, *Transport and Optical Properties of Nanomaterials—ICTOPON - 2009*, edited by M. R. Singh and R. H. Lipson